

Global wave energy resource classification system for regional energy planning and project development

Seongho Ahn^a, Vincent S. Neary^{a,*}, Kevin A. Haas^b

^a Water Power Technologies, Sandia National Laboratories, Albuquerque, NM, USA

^b School of Civil & Environmental Engineering, Georgia Tech, Atlanta, GA, USA



ABSTRACT

Efforts to streamline and codify wave energy resource characterization and assessment for regional energy planning and wave energy converter (WEC) project development have motivated the recent development of resource classification systems. Given the unique interplay between WEC absorption and resource attributes, viz., available wave power frequency, directionality, and seasonality, various consensus resource classification metrics have been introduced. However, the main international standards body for the wave energy industry has not reached consensus on a wave energy resource classification system designed with clear goals to facilitate resource assessment, regional energy planning, project site selection, project feasibility studies, and selection of WEC concepts or archetypes that are most suitable for a given wave energy climate. A primary consideration of wave energy generation is the available energy that can be captured by WECs with different resonant frequency and directional bandwidths. Therefore, the proposed classification system considers combinations of three different wave power classifications: the total wave power, the frequency-constrained wave power, and the frequency-directionally constrained wave power. The dominant wave period bands containing the most wave power are sub-classification parameters that provide useful information for designing frequency and directionally constrained WECs. The bulk of the global wave energy resource is divided into just 22 resource classes representing distinct wave energy climates that could serve as a common language and reference framework for wave energy resource assessment if codified within international standards.

1. Introduction

Energy resource classification systems appraise the resource within a region or site in terms of the opportunity for energy generation based mainly on the available annual average power density for energy production, but these systems can also include metrics on resource constraints and risks. The steps for developing energy resource classification systems are given in Ref. [1]. Once the classification metrics are selected, their values, spatial variation and variance within the region of interest are estimated from historic observations, e.g., wind reanalysis data for wind resource classification systems. The division of metric values into different classes through the delineation of threshold values separating them is determined in various ways: a combination of statistical thresholds and expert judgment to achieve some objective, e.g., a balanced spatial distribution of classes in the region commensurate with the geographic distribution of regional wave climate attributes, the anticipated WEC project types (ranging from high power density utility-scale to low power density alternative market projects), a purely objective cluster analysis, or some combination of these methods. These

resource classification systems are valuable tools that provide a common language for resource assessment and facilitate energy planning and project development studies. Examples include the wind energy resource classification systems, and their corresponding wind resource class maps and atlases, developed for the United States (US) [2] and Europe [3]. These classification systems have supported national and regional energy planning and numerous project development studies at reconnaissance and feasibility levels [4], including national wind resource assessments outside the US and Europe, e.g., Refs. [5–9]. A recent classification of the global ocean wind energy resource adopted the US classification system [7].

The success of these wind energy resource classification systems has motivated the development of wave energy resource classification systems (WERCS). Martinez and Iglesias [10] developed a WERCS based primarily on the 40-year mean total wave power (an integration of the energy over all frequencies and directions) assessed from the ERA-5 reanalysis database. This classification system distinguishes five power classes, from I to V, increasing in energy content where 10, 20, 40, 80 kW/m are defined as thresholds for each class. These power class

Abbreviations: WEC, Wave Energy Converter; US, United States; WERCS, Wave Energy Resource Classification System; O&M, Operation and Maintenance; WWIII, WaveWatch III®; CFSR, Climate Forecast System Reanalysis; TP, Total Power classification; FP, Frequency constrained Power classification; FDP, Frequency and Directionally constrained Power classification; IEC, International Electrotechnical Commission; CDF, Cumulative Distribution Functions.

* Corresponding author.

E-mail address: vsneary@sandia.gov (V.S. Neary).

<https://doi.org/10.1016/j.rser.2022.112438>

Received 19 October 2021; Received in revised form 26 January 2022; Accepted 4 April 2022

Available online 20 April 2022

1364-0321/© 2022 Elsevier Ltd. All rights reserved.

delineations are set to align with regional wave climate attributes, e.g., fetch distance, latitude, geography. A second classification metric, the *wave exploitability index*, similar to the inverse of a *relative risk ratio* proposed by others [11–14], is a measure of the opportunity for energy production relative to the risk to operations and survival due to extreme wave loads. For WEC development, however, knowledge of the total wave power may not be beneficial for common resonant-constrained and directionally dependent WECs operating in a narrow range of frequency and direction bands. In addition, this WERCS includes a disproportionate amount of deep ocean sites, heavily weighting classification to energetic sites. In fact, a greater resolution and weighting of relatively shallow coastal regions nearshore is needed as their close proximity to energy demand centers onshore avoids exorbitant project capital, operation and maintenance (O&M) costs [15].

Fairley et al. [16] proposed several WERCSs for the global coastal waters using multiple sets of wave climate parameters computed from a 12-year ERA-5 reanalysis database. These parameters include significant wave height, peak period, spectral width, directional width, and relative extreme wave height. Using a *K*-means clustering method, global coasts are divided into six *clusters* based on their wave parameters, and the *clusters* are defined as classes from 1 to 6 in order of increasing mean values of the significant wave height squared. As these classification systems are mainly based on the significant wave height and peak period, they do not capture the spatial distribution of the wave power, which is typically the primary metric in an energy resource classification system. Thresholds delineating the wave power classes are not defined. As a result, the ranges of the wave climate parameters within each class significantly overlap with those in other classes. This interplay between multiple parameters in the *K*-means clustering method obscures classification of the wave energy potential. Although the resource parameters considered in Fairley et al. [16] characterize the degree of constraints and risks for energy generation within different wave climates, they cannot quantitatively balance the classification of the energy potential (the most important energy resource classification parameter) with classes based on these secondary parameters. Consequently, their classification system is more suitable for classifying regional wave climates than wave energy resources.

Ahn et al. [17] developed WERCSs for coastal waters of the US using a 30-year Wave Watch III hindcast (ver. 5.08) [18], based on the total wave power, the dominant period band containing the most energy, and its frequency constrained wave power content. The wave energy resource is classified based on its energy content within the dominant period band, i.e., the *peak period band power class*, or, alternatively, as the total wave power, i.e., the *total power class*. Four power classes from I to IV decreasing in energy content were defined based on threshold values of 1.1, 5.7, and 22.8 kW/m, which correspond to the mean wave power for the US coasts and one standard deviation less and greater than this mean value. Three peak period band classes, from 1 to 3, with increasing peak periods (thresholds of 7 and 10 s), were also defined to resolve the dominant peak period band. While this initial class delineation was somewhat arbitrary, it was found to provide a reasonable geographic distribution of classes that corroborates with the geographic distribution of US regional wave climates. It was also judged to be a reasonable initial estimate of the power requirements for different types of WEC projects, e.g., high power generation utility-scale projects and low-power generation alternative market projects. The introduction of the *peak period band power class* was critical as the energy absorption by a WEC is maximized by resonating at the same frequency of the incident wave and generally constrained to a narrow frequency bandwidth [19, 20]. The *peak period band power class* within a given dominant period band provides essential information linked to the WEC's operating period bandwidth and optimal size [11]. Unlike the WERCSs developed by Fairley et al. [16], the available wave power constrained by the frequency spreading of energy was resolved and its magnitude was classified without incorporating other wave climate attributes.

All WERCSs developed to date do not account for the directionality of

wave power and are, therefore, limited to omni-directional or weathervaning WECs operating in a broad range of directional bands. Many WECs can only absorb the wave energy content within a narrow direction band by aligning normal to the direction of maximum directionally resolved wave power. Therefore, a WERCS should also provide information about the directionally resolved wave power associated with operating period bands to resolve the available wave power due to these constraints.

Herein, we develop a global WERCS for coastal waters by adopting the approach by Ahn et al. [17] using a validated 31-year global WaveWatch III model hindcast. However, additional classification and sub-classification parameters are included to resolve the frequency and directionally constrained wave power, i.e., the *directionally resolved peak period band power class* and *directionally resolved peak period band class*. The WERCS in the present study classifies the available wave power based on the three different levels of physical WEC constraints: level 1) the total wave power, i.e., the *total power class*, level 2) the frequency constrained wave power, i.e., the *peak period band power class* within a *dominant peak period band class*, and level 3) the frequency and directionally constrained wave power, i.e., the *directionally resolved peak period band class* within a *directionally resolved dominant peak period band class*.

The WERCS developed herein does not consider an index characterizing the temporal variability of the wave power as a classification parameter, which is a measure of a WEC project's capacity factor (the ratio of actual energy production to its rated power) and annual energy production. Nor does it consider an index characterizing extreme conditions, e.g., the relative risk ratio or exploitability index. While these indices are important and should be estimated as part of a thorough resource characterization and assessment study, they cannot quantitatively constrain the *annual average available wave power*, the main classification metric, like frequency and directional constraints. However, they can easily be added to the WERCS herein as subclassification parameters if desired to augment assessment of opportunities, constraints, and risks based on these important factors.

The present study is organized as follows: The data source and methodology are described in Section 2. The class parameters and the threshold values separating classes are defined in Sections 3 and 4. In section 5, the geographical distribution of the resource classes is mapped and compared with known trends in regional wave climate attributes. Section 6 discusses key findings relative to other classification studies, and practical aspects of utilizing the WERCS proposed herein to facilitate wave energy resource characterization and assessment for energy planning and project development.

2. Data

The WERCS developed herein was built on resource parameters computed using the validated phase II 31-year global hindcast from a 3rd generation spectral wave model, WaveWatch III® (WWIII), with a spatial resolution of 0.5° [21]. In the phase II model, the Ardhuin et al. [22] physics package and bias-corrected Climate Forecast System Reanalysis (CFSR) wind data [18] were used, while the phase I model (v3.14) used Tolman and Chalikov [23] physics package and uncorrected CFSR [24] wind data.

WWIII provides hourly spectral partitioned bulk parameters at all computational grid points, e.g., partitioned wave height, partitioned peak period, partitioned mean direction [25], and corresponding wind sea fraction. These partitioned bulk data were generated by a spectral partitioning process, which divides modeled frequency-directional wave spectrum into multiple partitions representing energy from sub-peaks within the spectrum using a watershed identification algorithm [26]. The model domain along with the 31-year averaged wave power computed from the partitioned bulk parameters is shown in Fig. 1 (a). Only 2500 wave sites close to the shoreline shown in Fig. 1 (b) are used to avoid the inadvertent overrepresentation of energetic sites in deep

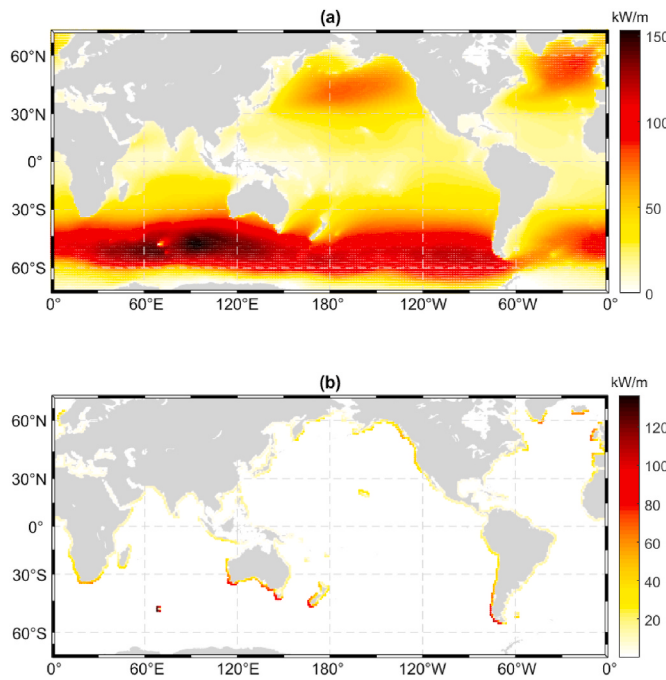


Fig. 1. (a) 31-year averaged global total wave power. (b) Study site locations along with the 31-year averaged total wave power.

oceans within the population and its power density frequency distribution. Pacific Islands except for Fiji, New Caledonia, and Solomon Islands are not considered in this study as the model did not resolve small islands due to the coarse spatial resolution.

3. Classification parameters

The WERCS developed herein includes classifications of the available wave energy based on the three different levels of physical WEC constraints listed in Table 1. The total power classification (hereinafter referred to as “TP”) classifies a wave site based on the total wave power without considering the physical constraints. The frequency constrained power classification (hereinafter referred to as “FP”) classifies a wave site based on the wave power content within a dominant peak period band. The frequency and directionally constrained power classification (hereinafter referred to as “FDP”) classifies a wave site based on the directionally resolved wave power content within a dominant peak period band. Note that the peak period band discriminates the physical range of a WEC’s resonant bandwidth, and the dominant peak period band is the peak period band containing the most wave power. The directionally resolved wave power is the sum of all wave power content propagating normal to a particular direction.

TP reflects the upper limit of available wave power unconstrained by the WEC’s limitations to absorb wave power in a narrow frequency and/or direction band. Although no WEC, even with advanced controls, can

absorb power in all frequency and direction bands, TP would best characterize the available wave power resource for an omni-directional WEC designed to have broadband resonance and an advanced control system to enhance this broadband performance. Similarly, FP, would best characterize the available wave power resource for an omni-directional WEC designed with a narrow resonance bandwidth and no advanced control system. FDP would best characterize the available wave power resource for a directionally-dependent WEC with broadband resonance enhanced with an advanced control system. Even for an omni-directional WEC with a broadband resonance bandwidth, it is important for the WERCS to include subclasses that indicate the resource’s dominant peak period band that contains the most wave power. The dominant directional property of the wave power is further refined by including the direction associated with the maximum directionally resolved wave power. In this section, definitions and computations of these class parameters are described.

3.1. Frequency-directionally resolved wave power distribution

As the resonant frequency band and directional dependency of a WEC can constrain the available power that it can capture, 31-year averaged joint wave power distributions in terms of the peak period and direction are computed for the study sites. The wave power transmitted by each partitioned wave, i.e., the partitioned wave power, J_n in kW/m, can be approximated as

$$J_n \approx \frac{\rho g}{16} H_{s,n}^2 C_{g,n} \quad (1)$$

by assuming that all the energy within the partition is transmitted at its group velocity ($C_{g,n}$) associated with the energy period ($T_{e,n}$). Where ρ is the sea-water density (1025 kg/m^3), g is the gravity acceleration (9.81 m/s^2), and $H_{s,n}$ is the partitioned significant wave height. To compute $C_{g,n}$, the partitioned energy period ($T_{e,n}$) is estimated using the partitioned peak period ($T_{e,n}$) based on a relationship, $T_e = CT_p$, which is derived from parametric spectrum models. In previous studies, various parametric spectrum models were used to estimate T_e when frequency wave spectra were not available [27]. Gunn and Williams [28] assumed $C = 0.86$ by adopting Pierson-Moskowitz spectrum [29]. Mestres and Jebbad [30], Sierra et al. [31], Gonçalves et al. [32], and Pastor and Liu [33] assumed $C = 0.9$ by adopting Joint North Sea Wave Project (JONSWAP) [34]. Some studies used a Gaussian spectrum [17] and assumed $C = 1.0$ [11,35,36] to represent a swell system [37,38]. In this study, we used $C = 0.86$ for wind sea and $C = 1.0$ for swell. The accuracy of the wave power computation using this combination was validated in Ahn et al. [17] for a broad range of US wave climates.

J_n spanning 31-year periods of record are sorted into peak period bins (T_b , resolution of 1 s) and direction bins (θ_b , resolution of 10° clockwise from the North) based on their partitioned peak period and direction. The 31-year averaged frequency-directionally resolved wave power distribution, $J(T_b, \theta_b)$, is computed as the summation of J_n pairs within the element (T_b, θ_b) divided by the number of hours in a 31-year (T) as

$$J(T_b, \theta_b) = \sum_1^N J_n / T \quad (2)$$

where N is the number of J_n paired in the element (T_b, θ_b) . This joint wave power distribution is analogous to the frequency-directional wave variance spectrum in that it resolves the theoretical wave energy resource within a particular wave period and direction [39]. An example of $J(T_b, \theta_b)$ for a wave site near Hawaii is shown in Fig. 2 (a), where $J(T_b, \theta_b)$ resolves two different dominant wave energy systems contributing the most energy to the total wave power. Long period (13–17 s) swells generated by North Pacific storms and short period (8–10 s) swells generated by the trade winds contribute similar wave energy for this site [40,41]. A unimodal WEC operating in a narrow period band could only

Table 1
Definition of classification parameters used in the present study.

Classification	Parameter	Sub-parameter
Total Power (TP)	Total wave power, J	–
Frequency constrained Power (FP)	Wave power within a dominant peak period band, $\max[J(\text{Band})]$	Dominant peak period band associated with $\max[J(\text{Band})]$, $\text{Band}_{\max[J(\text{Band})]}$
Frequency and Directionally constrained Power (FDP)	Directionally resolved wave power within a dominant peak period band, $\max[J(\text{Band})_{\theta_{\max}}]$	Dominant peak period band associated with $\max[J(\text{Band})_{\theta_{\max}}]$, $\text{Band}_{\max[J(\text{Band})_{\theta_{\max}}]}$

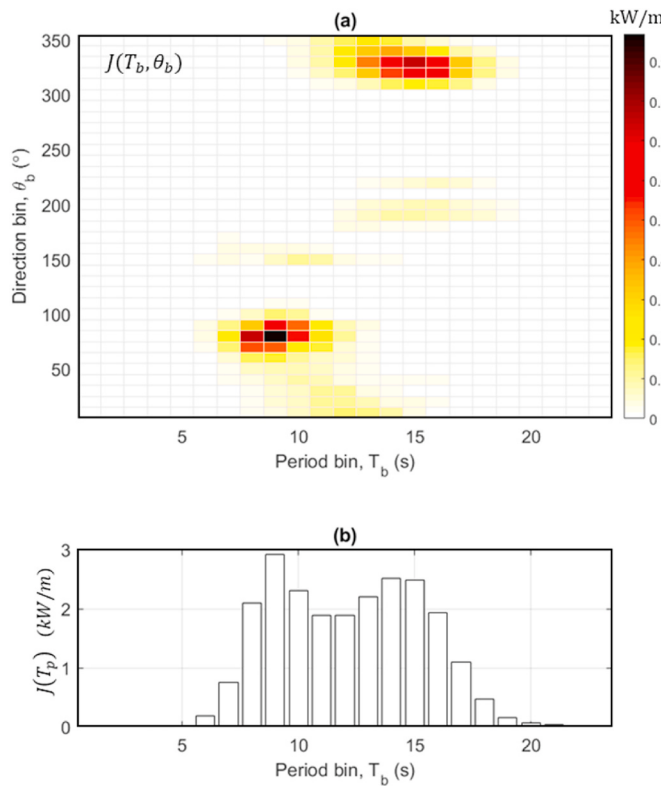


Fig. 2. (a) Example of 31-year averaged frequency-directionally resolved wave power distribution, $J(T_b, \theta_b)$ in kW/m, for Hawaiian wave site (Hawaii, 22°N 159°W). (b) Example of 31-year averaged frequency-resolved wave power distribution, $J(T_p)$, for the same site.

absorb energy one of these dominant wave systems.

3.2. Total wave power

The 31-year averaged total wave power, J , is simply the sum of all elements of $J(T_b, \theta_b)$ as

$$J = \sum_{T_b} \sum_{\theta_b} J(T_b, \theta_b) \quad (3)$$

The geographical distribution of J along the study sites is shown in Fig. 1 (b). The “Total Power Class” is defined based on J (see Section 4).

3.3. Peak period band (frequency constrained) wave power

The wave power as a function of the peak period bin, $J(T_b)$, is taken as the summation of power over all direction bins as $J(T_b) = \sum_{\theta_b} J(T_b, \theta_b)$ (e.g., Fig. 2 (b)). The wave power content in each peak period band, $J(Band)$, is computed by aggregating all $J(T_b)$ within that band. The frequency constrained power classification (FP) classifies the wave power within a dominant peak period band based on the maximum value of $J(Band)$ as

$$\max[J(Band)] = \max \left[\sum_{Band} J(T_b) \right] \quad (4)$$

where “Band” in Equation. 4 represents the peak period band (see Section 4.1).

3.4. Maximum directionally resolved period band wave power

The maximum directionally resolved $J(T_b)$, $J(T_b)_{\theta_{max}}$, propagating

through a vertical plane with the normal vector in direction θ (or WEC facing direction), is computed by adding each element of the $J(T_b, \theta_b)$ resolved in the direction θ as

$$J(T_b)_{\theta_{max}} = \max \left[\sum_{\theta_b} J(T_b, \theta_b) \cos(\theta_b - \theta) \delta \right] \quad (5)$$

where T_b is the period bin and θ_b is the direction bin as defined above. The direction θ used to find the maximum directionally resolved power has the same resolution as the direction bin θ_b . The parameter $\delta = 0$ for $\cos(\theta_b - \theta) \leq 0$ and $\delta = 1$ for $\cos(\theta_b - \theta) > 0$ to ensure that wave energy with positive elements in the direction contributes to $J(T_b)_{\theta}$. An example of $J(T_b)_{\theta}$ for the same site in Hawaiian coastal waters is provided in Fig. 3. $J(T_b)_{\theta_{max}}$ is analogous to “maximum directionally resolved wave power” recommended by the International Electrotechnical Commission (IEC) [42], but it captures the dependency of the period. This example shows that a directional WEC facing 80° and resonating at 9 s would experience the largest available wave power for this site.

Similarly, the maximum directionally resolved $J(band)$, $J(Band)_{\theta_{max}}$, is computed as

$$J(Band)_{\theta_{max}} = \max \left[\sum_{\theta_b} J(Band, \theta_b) \cos(\theta_b - \theta) \delta \right] \quad (6)$$

where “Band” represents the peak period band (see Section 4). The frequency and directionally constrained power classification (FDP) classifies the directionally resolved wave power within a dominant peak period band based on the maximum value of $J(Band)_{\theta_{max}}$. The direction associated with $\max[J(Band)_{\theta_{max}}]$ is also designated in this WERCS.

4. Class delineations

4.1. Dominant peak period band sub-class

The dominant peak period band, i.e., the peak period bin with the maximum wave power, is determined for all sites. Fig. 4 (a) shows the geographical distribution of dominant peak period bin, T_b in seconds, ranging from 2 - 5 s along sheltered and fetch-constrained coastal wave sites to 14 – 16 s along western coasts exposed to large swells generated from prevailing westerlies. Fig. 4 (b) shows the corresponding histogram with red-dashed lines delineating the dominant peak period bands at 6, 10, and 14 s. These threshold values were determined by applying this histogram to an algorithm initially developed for detecting abrupt

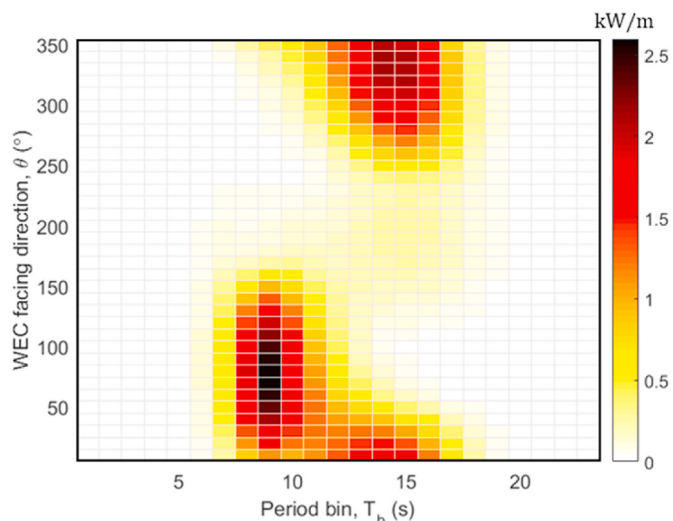


Fig. 3. Example of directionally resolved wave power as a function of peak period bin, $J(T_b)_{\theta}$ in kW/m, for the Hawaiian wave site.

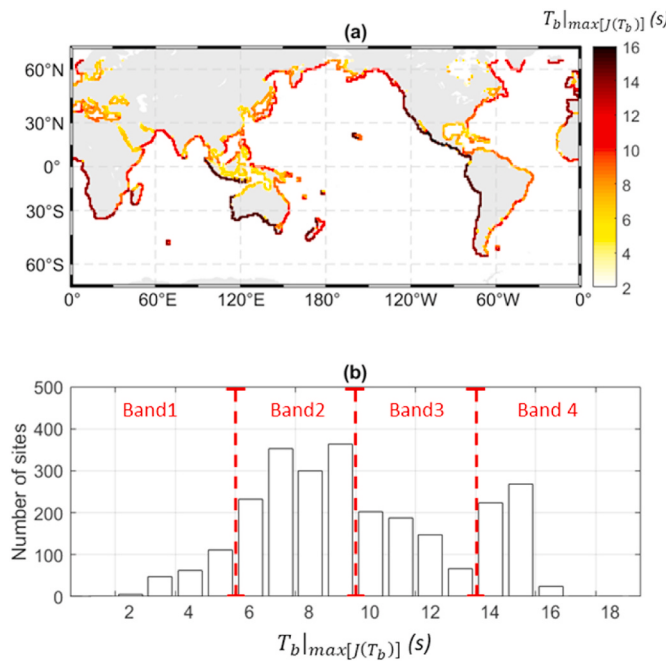


Fig. 4. (a) Geographical distribution of the dominant peak period bin, $T_b|_{max[J(T_b)]}$ in seconds, containing the maximum value of the frequency constrained wave power . (b) Frequency histogram of dominant peak period bin ($T_b|_{max[J(T_b)]}$) for coastal wave sites around the globe.

changes in signal [43]. This algorithm splits the histogram into four parts that minimize the sum of squared error of each part from its local mean.

Based on these threshold values, four peak period band sub-classes shown in Table 2 are defined to distinguish the dominant peak period bands with the most wave power for different regional wave climates observed around the globe. These thresholds delineate four-wave climates roughly corresponding to wind seas (Band 1), short-period swells (Band 2), intermediate period swells (Band 3), and long period swells (Band 4), which are generated by different prevailing wind climates for broad geographic regions. To maximize wave energy absorption of a WEC, especially those with narrow resonance bandwidths, would need to size their devices to resonate within these dominant peak period bands.

Based on the dominant peak period band sub-class ranges given in Table 2, $\max[J(Band)]$ and $\max[J(Band)_{\theta_{max}}]$ are computed and corresponding dominant peak period bands are sub-classified as FP and FDP. Fig. 5 shows J , $\max[J(Band)]$, and $\max[J(Band)_{\theta_{max}}]$ at the Hawaiian wave site. While $\max[J(Band)]$ is found in Band 3, $\max[J(Band)_{\theta_{max}}]$ is found in Band 2. Therefore, dominant peak period band sub-classes for FP and FDP are Band 3 and Band 2, respectively.

4.2. Power classes

Cumulative distribution functions (CDF) of computed values for each power class parameter at all study sites, J , $\max[J(Band)]$, and $\max[J(Band)_{\theta_{max}}]$, are shown in Fig. 6. The red line, CDF computed by combining the three power class parameters at all study sites, is used to delineate the thresholds (boundaries) between each power class as

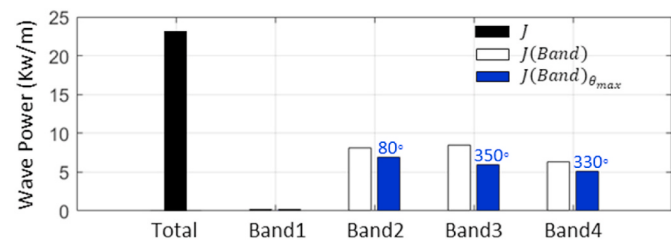


Fig. 5. Values of J , $\max[J(Band)]$, and $\max[J(Band)_{\theta_{max}}]$ along with direction associated with $\max[J(Band)_{\theta_{max}}]$ for the sample site.

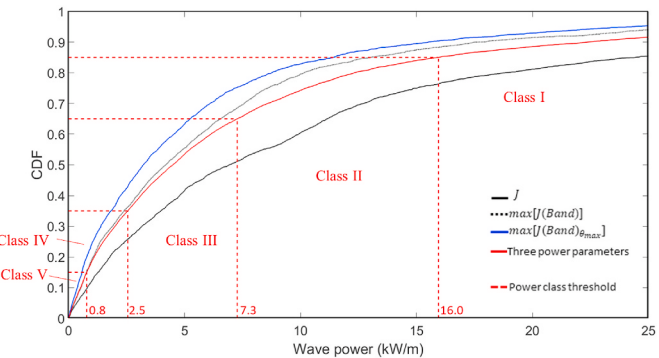


Fig. 6. Cumulative distribution functions derived from J , $\max[J(Band)]$, $\max[J(Band)_{\theta_{max}}]$ for all study sites and threshold values for the wave power classes.

shown in Table 3. These thresholds, 0.8, 2.5, 7.3, and 16 kW/m, selected to obtain a desirable geographic distribution of power classes that corroborates with our knowledge of regional wave climates, correspond to 15, 35, 65, and 85 percentiles of the combined CDF.

Fig. 7 supports the delineation of these threshold values showing percentages of sites in each class applying the three different power classifications (TP based on J , FP based on $\max[J(Band)]$, and FDP based on $\max[J(Band)_{\theta_{max}}]$). These threshold values are determined to balance the frequency distribution among classes and avoid over-weighting a particular class. The 15 and 85 percentiles result in the best balance between the percentage of sites in Class I and Class V applying TP (total power classification) and FDP (frequency and directionally constrained power classification). For example, the percentage of sites in both Class I applying FDP and Class V applying TP is around 10% (Fig. 7). Similarly, the 35 and 65 percentiles result in the best balance between the percentage of sites in Class II and Class IV applying TP and FDP. Most of the global coastal wave sites fall into Class III for all three power classifications. There are more energetic power class sites, e.g., Classes I and II, applying TP and less energetic power class sites, e.g., Classes IV and V, when applying FP and FDP, which constrains available power.

For the Hawaiian site example shown in Fig. 5, the total wave power (J) is Class I applying TP, the frequency constrained wave power ($\max[J(Band)]$) is Class II (in Band 3) applying FP classification, and the frequency and directionally constrained wave power ($\max[J(Band)_{\theta_{max}}]$) is Class III (in Band 2) applying FDP. These different power classifications are intended to allow the power class to be tailored (aligned) to the given WEC constraints, whether it be an idealized omni-directional broad- or multi-resonant WEC that can harvest the total wave power over all frequency and directional bands (upper limit), a WEC that may

Table 2
Definition of dominant peak period band sub-classes.

Class	Band 1	Band 2	Band 3	Band 4
Period, T_p (s)	$T_p \leq 6$	$6 < T_p \leq 10$	$10 < T_p \leq 14$	$14 < T_p$
Frequency, f_p (Hz)	$0.17 \leq f_p \leq 0.17$	$0.1 \leq f_p < 0.17$	$0.07 \leq f_p < 0.1$	$f_p < 0.07$

Table 3
Definition of power classes.

Class I	Class II	Class III	Class IV	Class V
Power > 16	$7.3 < \text{Power} \leq 16$	$2.5 < \text{Power} \leq 7.3$	$0.8 < \text{Power} \leq 2.5$	Power ≤ 0.8

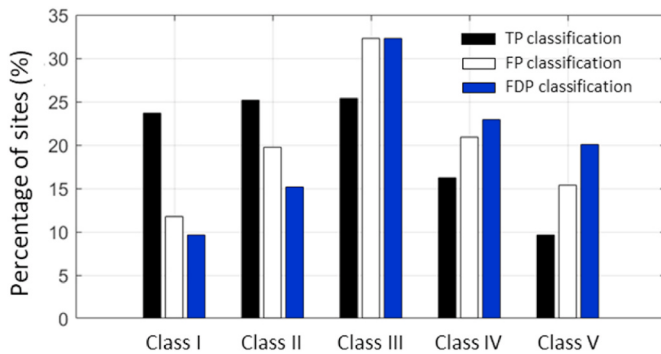


Fig. 7. Percentage of sites within each power class for the three classifications.

be frequency-constrained, or one that is both frequency- and directionally-constrained (lower limit). Comparisons with the previous WERCSs are provided in Section 6.

The average wave statistics and threshold values delineating classes can shift depending on the periods of record of the wave data. Using more recent shorter periods of record, while perhaps reducing uncertainty due to gradual nonstationary shifts in the wave climate, introduces larger uncertainty in WERCS because the global historical wave climate shows non-stationary trends with inter-annual or inter-decadal fluctuations, and these trends are not guaranteed to continue in the future [36,44,45]. Therefore, long-term wave data with multi-decadal periods of record are recommended to resolve average statistics of wave climates for the lifespan of WEC projects [42]. Nevertheless, understanding the uncertainties in historical nonstationary changes to regional wave climates remains a significant challenge and highlights the need to develop accurate methods for forecasting future trends. Average wave statistics and threshold values delineating classes need to be periodically verified with updated wave data to consider the climate changes.

5. Wave energy resource classification system

5.1. Geographic distribution of wave energy resource classes

The geographical distribution of the computed power classes for all coastal wave sites applying TP (total power classification), FP (frequency constrained power classification), and FDP (frequency and directionally constrained power classification) are plotted in Fig. 8 as a check to confirm that the power and dominant peak period band class delineations are selected to achieve a geographical distribution that corroborates with that of known regional wind and wave climate attributes observed around the globe. In general, the wave power at high latitude coasts dominated by prevailing westerlies is more energetic than low latitude coasts dominated by trade winds. The wave energy resource along western coasts of continents facing prevailing westerlies, e.g., the Pacific Northwest, the United Kingdom, western Europe, southwest South Africa, southwest Australia, southwest New Zealand, Chile, are classified as Class I for all three classifications. Coastal wave sites with the same class for the three classifications including the above regions comprise 30% of the total study sites and are listed in Table 4. Except for coastal wave sites in the Java Sea, the Banda Sea, and the Celebes Sea (Class V), the regions listed in Table 4 exhibit relatively large wave energy resources with a narrow frequency-directional spreading compared to other sites in each power class. These regions are exemplars for each class.

FP power classes at half the sites are lower than their respective TP power classes as they are constrained to the dominant peak period band. FP power classes along the eastern Pacific Ocean and the eastern Atlantic Ocean located between -30° and 30° latitude, e.g., Hawaii, western Mexico, Peru, western Africa, are one level reduction from their

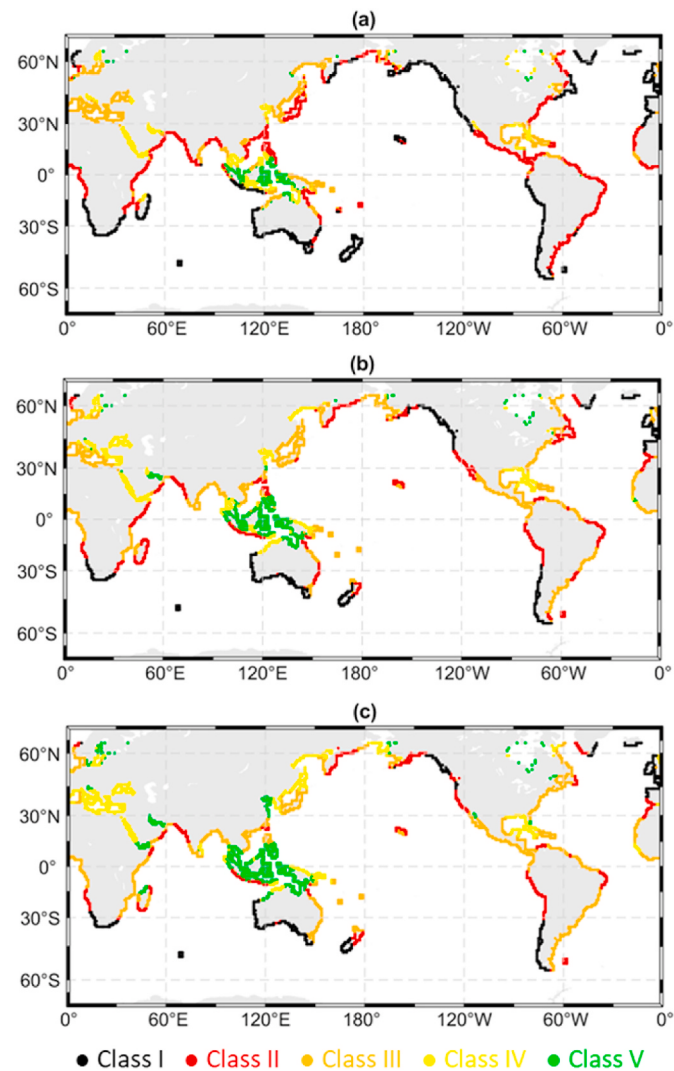


Fig. 8. Geographical distributions of (a) total power class in TP, (b) frequency constrained power class in FP, and (c) frequency and directionally constrained power class in FDP.

Table 4

Representative coastal regions, which are classified as the same class for all three power classifications.

Power Class	Coastal regions
I	Pacific Northwest, United Kingdom, western Europe, southwestern South Africa, southwestern Australia, southern New Zealand, Chile
II	northeastern Brazil, Arabian Sea, north Colombia
III	Western Gulf of Mexico, Dominican Republic, Venezuela, Gulf of Saint Lawrence, eastern South Korea, Bay of Bengal
IV	Central and eastern Gulf of Mexico, Red Sea
V	Java Sea, Banda Sea, Celebes Sea

TP power class (Fig. 8 (a) and (b)). However, at the middle latitude region between 30° and 60° in both hemispheres, the reduction in power class from TP to FP is mainly found in coasts along the western Pacific Ocean and the western Atlantic Ocean, e.g., Japan, Russia, US East Coast, and southeast coast of South America. Except for Hawaii, these reductions are mainly due to the wave climates in these regions having limited fetch as the prevailing westerlies and trade winds originate from land masses, resulting in relatively broad frequency spreading of the energy distribution [46]. Two dominant swell systems, trade wind

swells and westerly swells that contribute similar wave power to Hawaiian coasts, split into different period band sub-classes, Band 2 (trade wind swells) and Band 4 (westerly swells).

FDP power class at 26% of the sites is less than its FP power class as these sites are directionally constrained. This drop is most prevalent in enclosed or semi-enclosed seas, e.g., the Mediterranean Sea, Gulf of Aden, Gulf of Thailand, Solomon Sea, Yellow Sea, Sea of Japan, and the Bering Sea. Swells hardly reach these enclosed sheltered areas where the wave climates are generally dominated by seasonal wind seas from various directions in small fetch-limited ocean bodies. The broad directional spreading of wind seas within the short period band causes a significant reduction to FDP power classes for these regions.

Geographical distributions of the dominant peak period band sub-classes are shown in Fig. 9 (a) and (b). Most sites have the same period band sub-classes in FP and FDP. In general, the eastern sides of the Indian, Pacific, and Atlantic Oceans have most of their energy within longer period bands (Band 3 and 4) compared to the western sides of oceans (Band 2 and 3). This is mainly due to the global wave climates being more dominated by the prevailing westerlies than the trade winds where the swells reaching the eastern sides of oceans have longer fetches and periods compared to those of the western sites [47]. The eastern side of the South Atlantic Ocean has a shorter period band (Band 3), compared to the eastern side of other oceans (Band 4) due to their relatively short fetches that prevent long period swell generation. A WEC project at sites with Band 4 requires a relatively large WEC size, namely the mass of the prime mover of the oscillating body, to maximize energy capture by resonating at higher period waves. The wave energy resources at enclosed seas near Indonesia, e.g., Java Sea and Banda Sea, are within the short period band (Band 1) where relatively small-scale WEC applications can be considered. The dominant period band sub-classes in FP and FDP are not identical in some regions. FP period band sub-classes at the western Hawaii and southeastern Brazil are Band 3 and Band 2, while FDP period band sub-classes are in Band 4 and Band 3 (longer period band). Therefore, for these regions, a directionally dependent WEC would need to target the wave energy resource within

Band 4 or 3.

The geographical distribution of the direction associated with FDP, i.e., the direction containing the largest frequency and directionally constrained wave power, is shown in Fig. 10. A directionally dependent WEC would have to align normal to this direction to maximize energy absorption. Because the hindcast used in this study did not resolve complicated wave interactions and bathymetric gradients that affect the directionality of waves near the coasts [48], data from high-resolution wave models are required to assess directional information for regional energy planning and WEC design [42]. Although the direction shown in Fig. 10 may not be recommended for regional WEC projects, it is included herein to illustrate the benefits of a WERCS including this parameter.

5.2. Classification system

The wave energy resource classification system (WERCS) based on the three different classifications presented in Section 5.1 and the wave energy resource for the example wave site near Hawaii is classified in the schematic in Fig. 11. Assigned classes are listed from left to right in three registers separated by hyphens. The first register is the total power class in TP. The second register is the frequency constrained power class in FP and its corresponding dominant peak period band sub-class. The third register is the frequency and directionally constrained power class in FDP and its corresponding dominant peak period band sub-class, with its corresponding direction. The classification for the example site off the coast of Hawaii (Figs. 2, 3 and 5) is I-II(3)-III(2)80°. This classification system, while no substitute for a detailed resource characterization study, enables rapid assessment of the primary opportunities and constraints for regional energy planners, WEC project developers, and WEC designers.

While this five-parameter classification matrix includes 560 (35 × 4², 35 permutations of three power classifications and 4 peak period band sub-classes for each FP and FDP) resource classes (not including the direction parameter), a large majority of coastal wave sites around the globe (86%) fall within just 22 resource classes. These 22 resource classes are listed in Table 5 and their geographic distribution is mapped in Fig. 12. In Table 5, large coastal regions and nations associated with each resource class are specified based on the following criteria. First, large coastal regions classified as one resource class are specified (e.g., western Europe, West Africa). Second, nations with large coastal areas are specified (e.g., Brazil, Chile, South Africa). Third, nations with relatively small coastal areas are specified if their resource is classified as one resource class (e.g., Kenya, Morocco). This WERCS demonstrates the benefits of combining the different classifications, TP, FP, and FDP. Also, with just 22 resource classes (Class 1–22 in Table 5) representing most coastal wave sites, a simple indirect-addressing approach is introduced to map this five-parameter classification matrix in Fig. 12.

FP and FDP power classes of TP Class I sites range from Class I to Class III. Their dominant peak period band sub-classes range from Band 3 to Band 4 (Class 1–6). Although FDP power classes in I-I(3)-II(3) and I-II(3)-III(3) regions (Class 3 and 6) are relatively low compared to regions

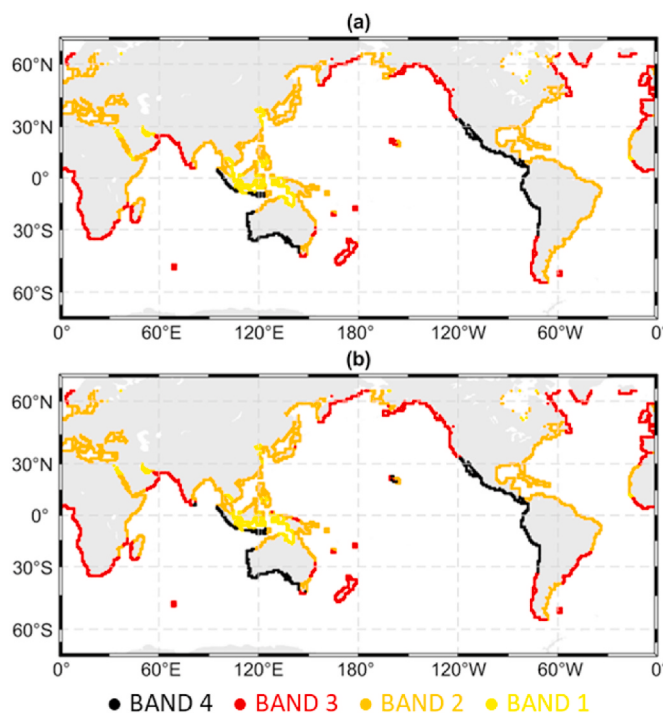


Fig. 9. Geographical distributions of (a) a dominant peak period band sub-class applying FP (frequency constrained power classification) and (b) a dominant peak period band sub-class applying FDP (frequency and directionally constrained power classification).

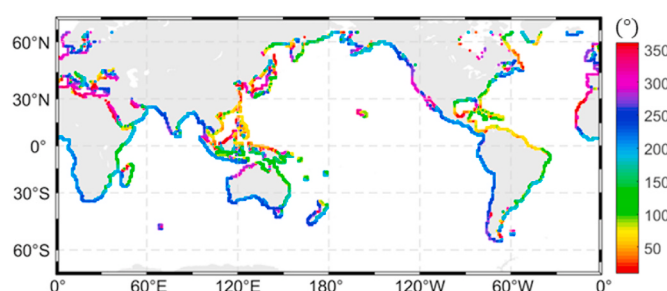
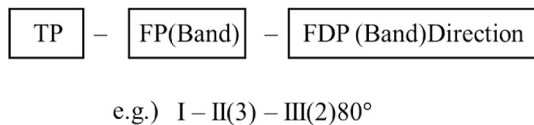


Fig. 10. Geographical distribution of the direction associated with FDP (frequency and directionally constrained power classification), i.e., the direction containing the largest frequency and directionally constrained wave power.



e.g.) I – II(3) – III(2)80°

Fig. 11. Classification system for wave energy resource incorporating all three classifications. An example for the classification of the wave energy resource for a wave site near Hawaii is included.

Table 5

Dominant global wave energy resource classes, the percentage of global coastal wave sites with these designated classifications, and the regions where these resource classes are observed. The color of the classification index represents the total wave power class listed in order from highest to lowest.

Index	Resource class(refer to Figure 11)	%	Coastal regions
1.	I – I(3) – I(3)	8.1	South Africa, south New Zealand, Chile, western Europe
2.	I – I(4) – I(4)	2.8	south and west Australia
3.	I – I(3) – II(3)	1.5	Northwest Pacific Ocean (west Canada, north California US)
4.	I – II(3) – II(3)	5.1	Namibia, northeast New Zealand, western Gulf of Alaska, Morocco
5.	I – II(4) – II(4)	2.2	Indian Ocean side of Indonesia, Peru, north Chile
6.	I – II(3) – III(3)	1.3	west Norway, east South Africa, east Canada
7.	II – II(2) – II(2)	1.7	south Taiwan, north Colombia, east Brazil
8.	II – II(3) – II(3)	1.5	Oman, Pakistan, west India
9.	II – II(2) – III(2)	2.5	Kenya, Somalia, northeast Philippines, northeast Brazil
10.	II – III(2) – III(2)	10.0	Japan, east US, northeast South America, Argentina, Mauritania
11.	II – III(2) – III(3)	1.4	Uruguay, southeast Brazil
12.	II – III(3) – III(3)	4.5	south India, Fiji, southern West Africa, Central Africa
13.	II – III(4) – III(4)	2.7	Pacific Ocean side of Mexico - Colombia
14.	III – III(2) – III(2)	6.2	South Korea, western Gulf of Mexico, Hispaniola, Venezuela
15.	III – III(2) – IV(2)	8.4	Mediterranean Sea, southeast India, southeast Russia
16.	III – IV(2) – IV(2)	7.6	Baltic Sea, Black Sea, Bismarck Sea, northern Sea of Okhotsk, Cuba
17.	IV – IV(2) – IV(2)	2.9	Adriatic Sea, Red Sea, eastern Gulf of Mexico
18.	IV – IV(1) – V(1)	1.5	north Persian Gulf, Cambodia, Yellow Sea
19.	IV – IV(2) – V(2)	2.3	Gulf of Bothnia, Gulf of Aden, South Thailand
20.	IV – V(1) – V(1)	2.3	south Persian Gulf, Arafura Sea
21.	V – V(1) – V(1)	4.7	Enclosed seas around Indonesia
22.	V – V(2) – V(2)	1.0	Enclosed seas around Indonesia

I-I(4)-I(4) and I-II(4)-II(4) (Class 2 and 5), the dominant energy in these regions (Class 3 and 6) is contained within the lower period band (Band 3). Therefore, smaller devices are more appropriate in these regions.

Although TP power class in Class 7–9 regions, Class II, is relatively low compared to that of Class 4–6 regions, Class I, we wouldn't conclude Class 7–9 regions have lower opportunities because they have similar energy for FP and FDP within shorter period bands. While TP, FP, and FDP power classes are identical for Class 10–13 regions, Class 10 regions have the shortest dominant peak period band, and thereby, all else being equal, a WEC project will require the smallest device in Class 10 regions. Class 11 regions are amenable to omni-directional and directionally dependent WECs designed to resonate at different period bands to maximize energy absorption.

Wave energy resource assessments that rely on the total available wave power fail to detect high opportunity project sites in Class 14–16 regions given their modest values for total wave power. However, the WERCS herein shows that FDP power class for these regions is Class III

and similar to Class 6 and Class 9–13 regions, which have a much higher TP power class than Class 14 regions. A common attribute of FDP power class for Class 14, Class 3–5, and Class 8 regions is their dominant energy is distributed within the shorter period band. TP, FP, and FDP power classes for Class 17–20 and Class 21–22 regions are Class IV and V where the most energy is within Bands 1 and 2. These regions are generally located in semi-enclosed or enclosed seas.

6. Discussion

6.1. Comparison with existing WERCS

As the global WERCS herein includes the total wave power classification (TP), it is similar to other published global WERCS [10,16], but the inclusion of additional classifications based on frequency and directionally constrained wave power are key improvements by accounting for frequency and directional constraints to wave energy capture. Like the WERCS of Fairley et al. [16] and Martinez and Iglesias [10], the higher power classes, Class I and II (TP) sites corresponding to Class 1–6 (Black) and Class 7–13 (Red) in Fig. 12, are mainly found in exposed regions of the Indian, Pacific, and Atlantic Oceans. The moderate energy class, Class III (TP), corresponding to Class 14–16 (Orange) in Fig. 12 and lower energy classes, Class IV and V (TP), Class 17–20 (Yellow) and Class 21–22 (Green) in Fig. 12, are found in semi-enclosed and enclosed seas with constrained fetch, respectively.

The WERCS developed herein discerns the opportunities for WEC project development at a more refined level by classifying frequency-directionally constrained wave power and identifying the dominant period band that contains the most energy. As mentioned earlier, the WERCS developed by Martinez and Iglesias [10] includes a disproportionate amount of energetic deep ocean sites, increasing the upper band and thresholds of total wave power class. As a result, their WERCS cannot discern distinct regional power classes for coastal waters. About 60% of coastal regions (those within approximately 50 km from the shore) fall into their lowest energy class (Class I, total wave power <10 kW/m), and only 1% of coastal regions fall into their largest energy class (Class V, total wave power >80 kW/m). Because their WERCS only considers total wave power as the measure of wave energy resource, it obscures more nuanced attributes of the wave energy climate. For example, while the WERCS developed by Martinez and Iglesias [10] classifies all US west coasts as Class III (20 kW/m < total wave power <40 kW/m), the WERCS developed herein distinguishes four different resource classes; the northern Pacific Northwest Coast is Class 1 (I-I(3)-I(3)) while the California Coast is Class 5 (I-II(4)-II(4)). It resolves spatial variations of regional wave climates of the US West Coast where North Pacific westerly swells reaching this region decrease southward and their peak period increases southward as they propagate further from their source [49]. The WERCS developed by Martinez and Iglesias [10] classifies the Arabian Sea and Bay of Bengal as Class II (10 < total wave power <20 kW/m). Although the total wave power in these regions is similar, the present study shows that the Arabian Sea exhibits larger frequency-directionally constrained wave power (FP and FDP) within the longer period band (Class 8, II-II(3)-II(3)) than the Bay of Bengal (Class 10, II-III(2)-III(2)).

The WERCSs developed for the US coastal waters [17] is based on the total wave power and frequency constrained wave power using four power classes (bounded by 1.1, 5.7, and 22.8 kW/m) and three peak period band classes (bounded by 7 s and 10 s). This delineation achieves a desirable geographic distribution of resource classes that corresponded with that of US wave energy climates. However, like the WERCS of Martinez and Iglesias [9], it also obscures sub-regional differences. Like the WERCS of Martinez and Iglesias [10], Ahn et al. [17] classifies the entire US West Coast using one power class (Class I, the highest energy class) based on both the total wave power and frequency constrained wave power. Wave energy resources associated with distinct regional wave climates are also resolved within the coastal waters of the Gulf of

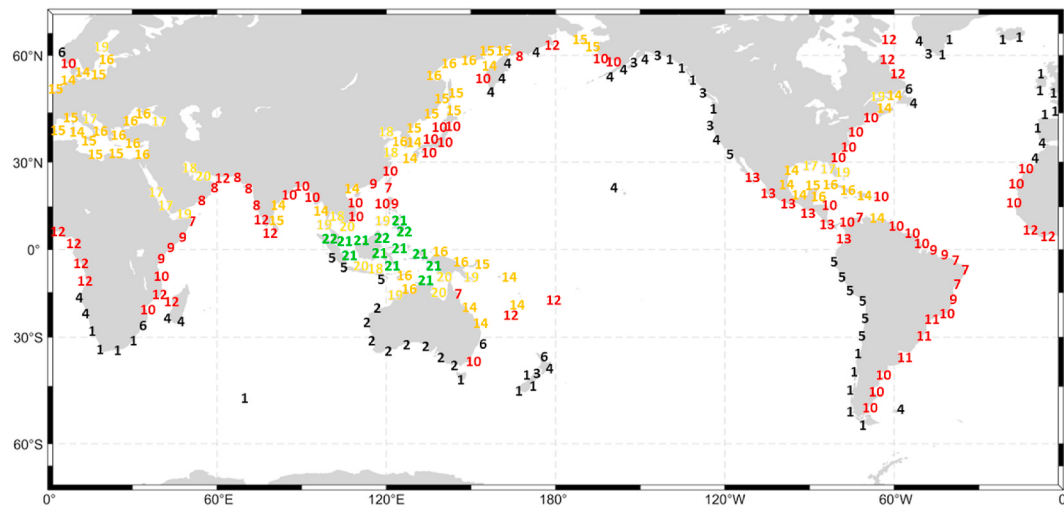


Fig. 12. Geographical distribution of classification indices (22 resource classes) listed in Table 5 where the color represents their total wave power class; black (TP Class I), red (TP Class II), orange (TP Class III), yellow (TP Class IV), green (TP Class V). Note that wave sites classified into resource classes having less than 1% of total wave sites within designated resource class, e.g., eastern Hawaii, are not shown in this figure. (For interpretation of the references to color in this figure legend, the reader is referred to the Web version of this article.)

Mexico by the WERCS developed in the present study; resources for the western and eastern Gulf of Mexico are Class 14 (III-III(2)-III(2)) and Class 17 (IV-IV(2)-IV(2)), while Ahn et al. [17] assigns just one class for the entire Gulf of Mexico.

Fairly et al. [16] developed seven WERCSs based on different combinations of wave climate parameters where thresholds of classes for each WERCS were different as they were automatically defined from K-means clustering algorithm. They delineate global wave climates by considering the various sets of wave parameters and show the similarities and differences between each classification. While their study is useful for wave energy resource characterization, it fails to convey these frequency and directional constraints that can affect wave power capture and absorption. The biggest drawback of their study is it uses significant wave height squared and peak period as the main classification parameters, rather than wave power. Although the significant wave height squared can be used as a relative measure of wave power, the main classification parameter for a WERCS should always be the available wave power. The threshold values of the wave power might be approximated using the significant wave height squared and peak period, but this introduces uncertainties as relations between the peak period and energy period from which the wave power can be computed vary spatially.

Because the WERCS recommended by Fairly et al. [16] ("WXSD") is based on eleven wave climate parameters, and not including the wave power, the classes are not in order of magnitude of the wave energy resource and the ranges of parameters within each class overlap significantly with other classes. For example, many sites classified as Class 1 and 2 (low energy classes in Fairly et al. [16]) have larger significant wave heights squared and peak periods than sites classified as Class 5 and 6 (high energy classes in Fairly et al. [16]). The approximate wave power of Class 3 (lower energy class in Fairly et al. [16]) is larger than that of Class 4 (higher energy class in Fairly et al. [16]), which is counter-intuitive. While wave sites along western South America generally have larger wave power than those on the eastern side, sites on the western side are Class 3 (lower energy class in Fairly et al. [16]) and those on the eastern side are Class 4 (higher energy class in Fairly et al. [16]).

6.2. Implication of the present WERCS

The newly added classification in the present WERCS, including frequency and directionally constrained wave power classification

(FDP), augments the classification at regions where there is pronounced spatial variation of the wave energy resource. This improvement is observed for wave energy resources along the Hawaiian coast. The spatial variation of the wave climate in this region is well known in terms of both frequency and directional energy distributions as multiple swells having different peak periods generated by North Pacific storms, trade winds, and South Pacific storms reach this region from different directions [50,51]. Fig. 13 shows that the WERCS herein discerns six different resource classes in this region. The geographic distribution of these resource classes illustrates spatial trends in both the north-south and west-east directions. TP, FP, and FDP power classes tend to be reduced southward and the corresponding dominant peak period bands tend to decrease eastward. The northwest sides (I-II(3)-II(3)340°) are more exposed to the longer period North Pacific storm swells from the northwest direction, while the southeast sides (II-III(2)-III(2)110°) are more exposed to the shorter period trade wind swells from the east direction [41]. The resource near south Hawaii that is sheltered from these swells is dominated by the longer period South Pacific storm swells and is Class II-III(3)-IV(4)190°. For comparison, the WERCSs developed by Martinez and Iglesias [10] and Ahn et al. [17] only capture the north-south trend and fail to resolve some of the essential wave energy climate attributes. This example demonstrates the ability of the WERCS herein to emulate the key attributes of regional wave energy resource climates as observed in previous investigations [40,41,51].

Another advantage of the WERCS developed herein is that it can identify WEC project opportunities even for moderate TP power class wave sites. Wave sites with the identical power classes applying TP, FP, and FDP, e.g., II-II-II, III-III-III, exhibit narrow frequency-directional energy spreading, which is desirable due to the high costs associated with capturing wave power over a broad frequency and directional range. For example, sites within Class 14 (III-III(2)-III(2)), e.g., coastal waters near eastern South Korea and the western Gulf of Mexico, are low power classes based on the total wave power, and therefore, would appear to have limited opportunities for WEC projects. However, their frequency-directionally constrained wave power is similar to wave sites in coastal waters at eastern South Africa and eastern Canada (I-II(3)-III(3)).

The present WERCS reduces descriptions of complex global wave energy climates to essential attributes and then organizes them into like-groups, which facilitates better understanding and knowledge of the opportunities and constraints for a WEC project development in a region. The resource classes in the WERCS representing different resource

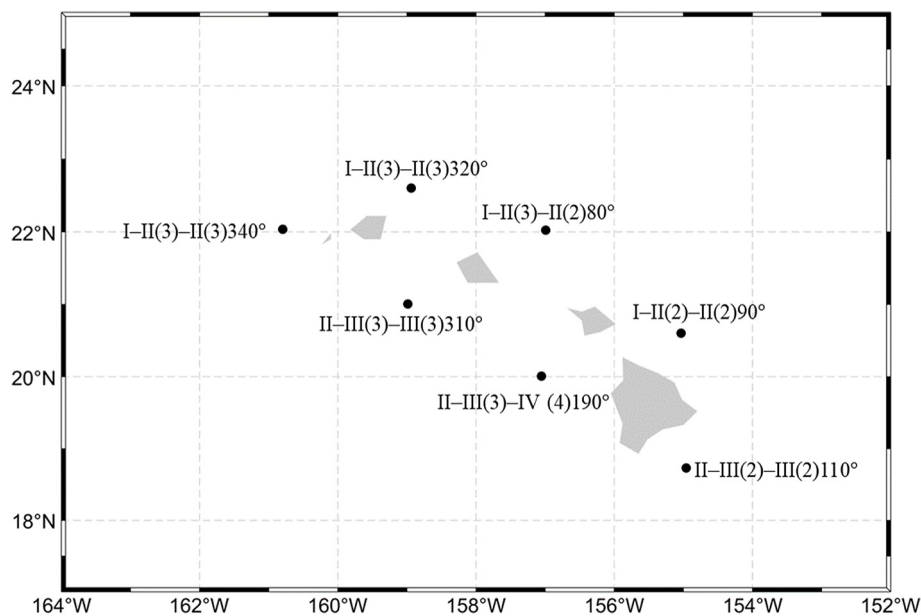


Fig. 13. Geographical distribution of wave energy resource classes around Hawaii.

attributes facilitate site selection, and reconnaissance and feasibility studies for project development, as well as WEC archetype selection and conceptual design. Similar WEC designs and O&M strategies can be applied to wave sites falling within the same resource class, potentially leading to a decrease in the cost. In this vein, the present WERCS ultimately contributes to reaching a consensus on what type of WEC is the most promising and appropriate for the wave energy market in the given region.

7. Conclusion

A novel wave energy resource classification system (WERCS) for global coastal wave sites is developed in the present study based on three available wave power classifications with a total of five parameters: Classification 1 based only on the total omni-directional (frequency and directionally unconstrained) wave power, Classification 2 based on the frequency constrained wave power and its dominant peak period band containing this power, and Classification 3 based on the frequency-directionally constrained wave power and its dominant peak period band containing this power. Combining all three classifications results in a five-parameter classification matrix that delineates distinct global wave energy resource classes.

The design intention of this WERCS is to have Classification 2 and 3 account for physical constraints of wave energy generation due to the potentially narrow resonance and directional capture bandwidths of common WECs. This system enables WEC designers to identify opportunities and constraints for project development, distinguish different wave energy capture and absorption strategies, and compare wave sites exhibiting desirable resource attributes for the given WEC constraints. This high-fidelity classification system includes the following highlights:

- although the five-parameter classification matrix results in 560 resource classes most coastal wave sites around the globe (86%) lie within just twenty-two resource classes.
- the geographical distribution of these resource classes, a resource classification map, represents different wave energy resource climates, which significantly streamline regional resource assessment and characterization.
- the degree of the constrained wave power is not proportional to that of the total wave power and coastal regions known to have low

energy are revalued based on the constrained wave power that can be absorbed by frequency and directionally constrained WECs.

Although there are other indices, e.g., the temporal variability and extreme wave conditions, which should be considered in assessing project opportunities, constraints, and risks, the WERCS developed herein focuses on the primary measure of available wave energy resource, wave power, which is the most important consideration for WEC project development. Indices characterizing temporal variability cannot quantitatively constrain the *annual average available wave power*, the main classification metric, like frequency and directional constraints. Examples above show that caution is warranted when mixing the resource classification with multiple wave climate parameters because the interplay between these summary parameters could obscure the classification of the available wave energy resource.

The WERCS herein can easily be extended by adding other indices as subclassification parameters to augment assessment of the opportunities, constraints, and risks based on these important factors. However, whether this extension from one parameter (wave power) to multiple-parameter classification system is warranted, deserves further consideration. On the one hand, there is value in maintaining a simple classification system focused on the available wave power in which the geographic distribution of resource classes shows clear trends; especially given the classification system is not meant to replace a thorough resource characterization and assessment study. On the other hand, indices characterizing temporal variability and extreme conditions may be so important that they should be codified in classification.

Author contribution

S. Ahn, V.S. Neary, K.A. Haas: Conceptualization, Methodology, S. Ahn: Data curation, Writing- Original draft preparation. S. Ahn, V.S. Neary: Analysis, Investigation. V.S. Neary: Supervision, Funding acquisition, Project administration V.S. Neary, K.A. Haas: Writing- Reviewing and Editing.

Declaration of competing interest

The authors declare that they have no known competing financial interests or personal relationships that could have appeared to influence the work reported in this paper.

Acknowledgment

The present study was supported by Sandia National Laboratories. Sandia National Laboratories is a multi-mission laboratory managed and operated by National Technology and Engineering Solutions of Sandia, LLC., a wholly owned subsidiary of Honeywell International, Inc., for the U.S. Department of Energy's National Nuclear Security Administration under contract DE-NA0003525. This paper describes objective technical results and analysis. Any subjective views or opinions that might be expressed in the paper do not necessarily represent the views of the U.S. Department of Energy or the United States Government.

References

- [1] Neary VS, Haas KA, Colby JA. Marine energy classification systems: tools for resource assessment and design. In: Proc. 13th Eur. Wave Tidal Energy Conf.; 2019. Naples, Italy.
- [2] Elliott DL, Holliday CG, Barchet WR, Foote HP, Sandusky W. Wind energy resource atlas of the United States. 1986. <https://doi.org/10.5860/choice.41-2192>. DE8600442. Richland, WA (USA).
- [3] Troen I, Lundtang Petersen E. European wind atlas. 1989.
- [4] Manwell JF, McGowan JG, Rogers AL. Wind energy explained: theory, design and application. Wiley Press; 2010.
- [5] Habali SM, Amr M, Saleh I, Ta'Ani R. Wind as an alternative source of energy in Jordan. Energy Convers Manag 2001;42:339–57. [https://doi.org/10.1016/S0196-8904\(00\)0054-6](https://doi.org/10.1016/S0196-8904(00)0054-6).
- [6] Ilincă A, McCarthy E, Chaumel J-L, Rétrieau J-L. Wind potential assessment of Quebec Province. Renew Energy 2003;28:1881–97. [https://doi.org/10.1016/s0960-1481\(03\)00072-7](https://doi.org/10.1016/s0960-1481(03)00072-7).
- [7] Zheng CW, Pan J. Assessment of the global ocean wind energy resource. Renew Sustain Energy Rev 2014;33:382–91. <https://doi.org/10.1016/j.rser.2014.01.065>.
- [8] Chen X, Foley A, Zhang Z, Wang K, O'Driscoll K. An assessment of wind energy potential in the Beibu Gulf considering the energy demands of the Beibu Gulf Economic Rim. Renew Sustain Energy Rev 2020;119:109605. <https://doi.org/10.1016/j.rser.2019.109605>.
- [9] Vinhoza A, Schaeffer R. Brazil's offshore wind energy potential assessment based on a Spatial Multi-Criteria Decision Analysis. Renew Sustain Energy Rev 2021;146:111185. <https://doi.org/10.1016/j.rser.2021.111185>.
- [10] Martinez A, Iglesias G. Wave exploitability index and wave resource classification. Renew Sustain Energy Rev 2020;134:110393. <https://doi.org/10.1016/j.rser.2020.110393>.
- [11] Neary VS, Coe RG, Cruz J, Haas K, Bacelli G, Debruyne Y, et al. Classification systems for wave energy resources and WEC technologies. Int Mar Energy J 2018;1:71–9.
- [12] Neary VS, Ahn S, Seng BE, Allahdadi MN, Wang T, Yang Z, et al. Characterization of extrenewave conditions for wave energy converter design and project risk assessment. J Mar Sci Eng 2020;8:1–19. <https://doi.org/10.3390/JMSE8040289>.
- [13] Reguero BG, Losada IJ, Méndez FJ. A global wave power resource and its seasonal, interannual and long-term variability. Appl Energy 2015;148:366–80. <https://doi.org/10.1016/j.apenergy.2015.03.114>.
- [14] Hiles CE, Robertson B, Buckingham BJ. Extreme wave statistical methods and implications for coastal analyses. Estuar Coast Shelf Sci 2019;223:50–60. <https://doi.org/10.1016/j.ecss.2019.04.010>.
- [15] Foley MJ, Whittaker TJT. Analysis of the nearshore wave energy resource. Renew Energy 2009;34:1709–15. <https://doi.org/10.1016/j.renene.2009.01.003>.
- [16] Fairley I, Lewis M, Robertson B, Hemer M, Masters I, Horrillo-Caraballo J, et al. A classification system for global wave energy resources based on multivariate clustering. Appl Energy 2020;262:114515. <https://doi.org/10.1016/j.apenergy.2020.114515>.
- [17] Ahn S, Haas KA, Neary VS. Wave energy resource classification system for US coastal waters. Renew Sustain Energy Rev 2019;104:54–68. <https://doi.org/10.1016/j.rser.2019.01.017>.
- [18] National Oceanic and Atmospheric Administration. In: WAVEWATCH III® Hindcast and reanalysis Archives. Natl Ocean Atmos Adm; 2020. <http://polar.ncep.noaa.gov/waves/hindcasts/>.
- [19] Drew B, Plummer AR, Sahinkaya MN. A review of wave energy converter technology. Proc Inst Mech Eng Part A J Power Energy 2009;223:887–902. <https://doi.org/10.1243/09576509JPE782>.
- [20] Korde UA. Efficient primary energy conversion in irregular waves. Ocean Eng 1999;26:625–51. [https://doi.org/10.1016/S0029-8018\(98\)00017-1](https://doi.org/10.1016/S0029-8018(98)00017-1).
- [21] Chawla A, Spindler DM, Tolman HL. Validation of a thirty year wave hindcast using the Climate Forecast System Reanalysis winds. Ocean Model 2013;70:189–206. <https://doi.org/10.1016/j.ocemod.2012.07.005>.
- [22] Ardhuin F, Rogers E, Babanin AV, Filipot JF, Magne R, Roland A, et al. Semiempirical dissipation source functions for ocean waves. Part I: definition, calibration, and validation. J Phys Oceanogr 2010;40:1917–41. <https://doi.org/10.1175/2010JPO4324.1>.
- [23] Tolman HL, Chalikov D. Source terms in a third-generation wind wave model. J Phys Oceanogr 1996;26:2497–518. [https://doi.org/10.1175/1520-0485\(1996\)026<2497:STIATG>2.0.CO;2](https://doi.org/10.1175/1520-0485(1996)026<2497:STIATG>2.0.CO;2).
- [24] Saha S, Moorthi S, Pan HL, Wu X, Wang J, Nadiga S, et al. The NCEP climate forecast system reanalysis. Bull Am Meteorol Soc 2010;91:1015–57. <https://doi.org/10.1175/2010BAMS3001.1>.
- [25] Tolman HL. User manual and system documentation of WAVEWATCH-III version 3.14. 2009.
- [26] Vincent L, Soille P. Watersheds in digital spaces: an efficient algorithm based on immersion simulations. IEEE Trans Pattern Anal Mach Intell 1991;13:583–98. <https://doi.org/10.1109/34.87344>.
- [27] Ahn S. Modeling mean relation between peak period and energy period of ocean surface wave systems. Ocean Eng 2021;228:108937. <https://doi.org/10.1016/j.oceaneng.2021.108937>.
- [28] Gunn K, Stock-Williams C. Quantifying the global wave power resource. Renew Energy 2012;44:296–304. <https://doi.org/10.1016/j.renene.2012.01.101>.
- [29] Pierson WJ, Moskowitz L. A proposed spectral form for fully developed wind seas based on the similarity theory of S. A. Kitaigorodskii. J Geophys Res 1964;69:5181–90.
- [30] Mestres M, Jebbad R. Wave energy potential along the Atlantic coast of Morocco. Renew Energy 2016;96:20–32. <https://doi.org/10.1016/j.renene.2016.04.071>.
- [31] Sierra JP, Mössö C, Gonz D. Wave energy resource assessment in Menorca (Spain). Renew Energy 2014;71:51–60. <https://doi.org/10.1016/j.renene.2014.05.017>.
- [32] Gonçalves M, Martinho P, Soares CG. Assessment of wave energy in the canary islands. Renew Energy 2014;68:774–84. <https://doi.org/10.1016/j.renene.2014.03.017>.
- [33] Pastor J, Liu Y. Wave climate resource analysis based on a revised gamma spectrum for wave energy conversion technology. Sustainability 2016;8:1321–34. <https://doi.org/10.3390/su8121321>.
- [34] Hasselmann K, Barnett TP, Bouws E, Carlson H, Cartwright DE, Enke K, et al. Measurements of wind-wave growth and swell decay during the Joint North Sea Wave project (JONSWAP). Ergänzungsheft 1973;13(A).
- [35] Ahn S, Haas KA, Neary VS. Wave energy resource characterization and assessment for coastal waters of the United States. Appl Energy 2020;267. <https://doi.org/10.1016/j.apenergy.2020.114922>.
- [36] Ahn S, Neary VS. Non-stationary historical trends in wave energy climate for coastal waters of the United States. Ocean Eng 2020;216:108044. <https://doi.org/10.1016/j.oceaneng.2020.108044>.
- [37] Lucas C, Soares CG. On the modelling of swell spectra. Ocean Eng 2015;108:749–59. <https://doi.org/10.1016/j.oceaneng.2015.08.017>.
- [38] Holthuijsen LH. Waves in oceanic and coastal waters. Cambridge University Press; 2007.
- [39] Ahn S. Wave energy resource characterization and classification for the United States & numerical simulation of coastal circulation near point sal. Georgia Institute of Technologies; 2019.
- [40] Vitousek S, Barbee MM, Fletcher CH, Richmond BM, Genz AS. Coastal hazard analysis report. 2009.
- [41] Ahn S, Haas KA, Neary VS. Dominant wave energy systems and conditional wave resource characterization for coastal waters of the United States. Energies 2020;13:3041. <https://doi.org/10.3390/en13123041>.
- [42] International IEC. Standard, Marine energy – wave, tidal and other water current converters – Part 101: wave energy resource assessment and characterization. Geneva, Switzerland: Edition 1.0: 2015. IEC 62600-101.
- [43] Killick R, Fearnhead P, Eckley IA. Optimal detection of change points with a linear computational cost. J Am Stat Assoc 2012;107:1590–8. <https://doi.org/10.1080/01621459.2012.737745>.
- [44] Young IR, Vinoth J, Zieger S, Babanin AV. Investigation of trends in extreme value wave height and wind speed. J Geophys Res Ocean 2012;117. <https://doi.org/10.1029/2011JC007753>.
- [45] Reguero BG, Losada IJ, Méndez FJ. A recent increase in global wave power as a consequence of oceanic warming. Nat Commun 2019;1–14. <https://doi.org/10.1038/s41467-018-08066-0>.
- [46] Hurdal DP, Van Vledder GP. Improved spectral wave modelling of white-capping dissipation in swell sea systems. Proc Int Conf Offshore Mech Arct Eng - OMAE 2004;2:539–44. <https://doi.org/10.1115/OMAE2004-51562>.
- [47] Ahn S, Neary VS, Allahdadi MN, He R. Nearshore wave energy resource characterization along the East Coast of the United States. Renew Energy 2021. <https://doi.org/10.1016/j.renene.2021.03.037>.
- [48] Cavaleri L, Abdalla S, Benetazzo A, Bertotti L, Bidlot JR, Breivik, et al. Wave modelling in coastal and inner seas. Prog Oceanogr 2018;167:164–233. <https://doi.org/10.1016/j.pocean.2018.03.010>.
- [49] Ahn S, Neary VS. Wave energy resource characterization employing joint distributions in frequency-direction-time domain. Appl Energy 2021;285:116407. <https://doi.org/10.1016/j.apenergy.2020.116407>.
- [50] Stopa JE, Cheung KF, Chen Y-L. Assessment of wave energy resources in Hawaii. Renew Energy 2011;36:554–67. <https://doi.org/10.1016/j.renene.2010.07.014>.
- [51] Stopa JE, Filipot J-F, Li N, Cheung KF, Chen Y-L, Vega L. Wave energy resources along the Hawaiian Island chain. Renew Energy 2013;55:305–21. <https://doi.org/10.1016/j.renene.2012.12.030>.